

Conf- 901105--125

UCRL-JC-104530  
PREPRINT

*Received by OSTI*

JUN 1 0 1991

ACTINIDE TRANSPORT IN TOPOPAH SPRING TUFF: 0  
PORE SIZE, PARTICLE SIZE AND DIFFUSION

Marilyn Buchholtz ten Brink  
Douglas L. Phinney  
David K. Smith

This paper was prepared for submittal to  
Materials Research Society, Boston, MASS  
November 27-29, 1990 and publication in  
"Scientific Basis for Nuclear Waste Management  
XIV".

Manuscript Date: December 1990  
Publication Date: April 1991

Lawrence  
Livermore  
National  
Laboratory

This is a preprint of a paper intended for publication in a journal or proceedings. Since changes may be made before publication, this preprint is made available with the understanding that it will not be cited or reproduced without the permission of the author.

MASTER

ok

DISTRIBUTION OF THIS DOCUMENT IS UNLIMITED

## DISCLAIMER

This document was prepared as an account of work sponsored by an agency of the United States Government. Neither the United States Government nor the University of California nor any of their employees, makes any warranty, express or implied, or assumes any legal liability or responsibility for the accuracy, completeness, or usefulness of any information, apparatus, product, or process disclosed, or represents that its use would not infringe privately owned rights. Reference herein to any specific commercial products, process, or service by trade name, trademark, manufacturer, or otherwise, does not necessarily constitute or imply its endorsement, recommendation, or favoring by the United States Government or the University of California. The views and opinions of authors expressed herein do not necessarily state or reflect those of the United States Government or the University of California, and shall not be used for advertising or product endorsement purposes.

# ACTINIDE TRANSPORT IN TOPOPAH SPRING TUFF: PORE SIZE, PARTICLE SIZE, AND DIFFUSION

MARILYN BUCHHOLTZ TEN BRINK<sup>a</sup>, DOUGLAS L. PHINNEY<sup>b</sup>, and DAVID K. SMITH<sup>a</sup>  
Earth Sciences Department<sup>a</sup> and Nuclear Chemistry Division<sup>b</sup>  
Lawrence Livermore National Laboratory, L202, P.O. Box 808, Livermore, CA 94550.

UCRL-JC--104530  
DE91 013515

## ABSTRACT

Diffusive transport rates for aqueous species in a porous medium are a function of sorption, molecular diffusion, and sample tortuosity. With heterogeneous natural samples, an understanding of the effect of multiple transport paths and sorption mechanisms is particularly important since a small amount of radioisotope traveling via a faster-than-anticipated transport path may invalidate the predictions of transport codes which assume average behavior. Static-diffusion experiments using aqueous  $^{238}\text{U}$  tracer in tuff indicated that U transport was faster in regions of greater porosity and that apparent diffusion coefficients depended on the scale (mm or  $\mu\text{m}$ ) over which concentration gradients were measured in Topopah Spring Tuff. If a significant fraction of actinides in high-level waste are released to the environment in forms that do not sorb to the matrix, they may be similarly transported along fast paths in porous regions of the tuff. To test this, aqueous diffusion rates in tuff were measured for  $^{238}\text{U}$  and  $^{239}\text{Pu}$  leached from doped glass. Measured transport rates and patterns were consistent in both systems with a dual-porosity transport model. In addition, filtration or channelling of actinides associated with colloidal particles may significantly affect the radionuclide transport rate in Topopah Spring tuff.

## INTRODUCTION

Diffusive transport rates for aqueous species in a porous medium are a function of sorption, molecular diffusion, and sample tortuosity. Single constant values for these parameters result in transport that can be modelled as Fickian diffusion with one diffusion coefficient. With heterogeneous natural samples, however, an understanding of the effect of multiple transport paths and sorption mechanisms is particularly important when designing hazardous waste repositories, since a small amount of radioisotope traveling via a faster-than-anticipated transport path may invalidate the predictions of transport codes which assume homogeneous behavior.

Apparent diffusion coefficients ( $D_{\text{app}}$ ) for an aqueous species in a porous medium, such as the tuff from Yucca Mtn., Nevada, can be calculated either from concentration changes in the bulk solution after passage through the medium or from concentration profiles measured in the porous medium. Values derived from bulk-solution concentrations are averages over the entire sample and provide no information about the spatial variability of transport rates and concentrations within the sample. In the second approach, however, the scale of concentration gradients and variability is limited only by the spatial resolution of the technique selected for analysis. This solid-analysis approach is particularly useful for determining transport of strongly sorbing species, since either very long experiment times or short diffusion paths are needed to produce measurable changes in the bulk-solution concentration and because most of the species of interest stay with the solid phase. In this paper, we present results from two static-diffusion experiments (8 hours and 183 days in length) in which actinide elements migrated from solution into samples of tuff rock. In particular, the effect of variations in porosity and the presence of micro-fractures in the solid on the transport of radioisotopes is considered.

## METHODS

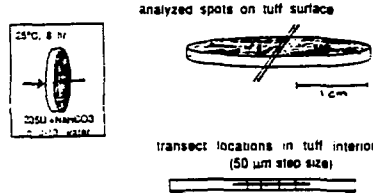
Details of the experimental conditions are given in McKeegan et al.<sup>1</sup> for the "tuff wafer" experiment and in Bazan, Rego and Aines<sup>2</sup> for the "tuff-cup" experiment. The rocks in both experiments were from the Topopah Spring member of the Paintbrush tuff, Nevada, which is the potential horizon for the Yucca Mountain high-level waste repository. Topopah Spring tuff is a fine-grained devitrified tuff with heterogeneous mineralogy and porosity<sup>3,1</sup>. The disks of tuff used in the "wafer" experiments were obtained from drill core (USWH-6), machined to size (2.45 cm diameter x 2 mm thickness), cleaned, polished on one face, and partially saturated to

approximately 70% saturation by immersion in J-13 groundwater prior to the experiment. The rock for the "tuff cup" experiments was obtained from surface outcrop at Fran Ridge and machined to form a vessel having a cylindrical interior of 6 cm x 2.5 cm diameter with walls and floor approximately 1.25 cm thick. The vessels were cleaned to remove surface salt deposits and saturated by immersion prior to use.

For both experiments, actinide-bearing solutions were allowed to diffuse into the tuff; however, the solutions and the experimental conditions differed. Briefly,  $^{235}\text{U}$  was equilibrated with J-13 groundwater (which is saturated with respect to the minerals in Topopah Spring tuff) and  $\text{NaHCO}_3$  buffer in preparation for measurement of U diffusion in tuff wafers. The solution, 2 ppm  $^{235}\text{U}$  with initial pH 7.2, was contained in a polyethylene (HDLPE) vial with a stainless-steel support for the tuff wafer. The tuff wafer was removed from the J13 water and immediately immersed in this solution for 8 hours at 25°C during which diffusion of  $^{235}\text{U}$  into the tuff occurred. It was then removed from solution, air-dried and prepared for analysis. In the tuff-cup experiment, pieces of ATM-8 borosilicate glass containing  $^{237}\text{Np}$ ,  $^{239}\text{Pu}$ ,  $^{99}\text{Tc}$ , and  $^{238}\text{U}$  were placed in J-13 groundwater on a teflon support inside the tuff vessel to provide an actinide source. The vessel was itself set in a teflon jar and surrounded with tuff-equilibrated groundwater. The actinide-bearing solution was allowed to diffuse through the tuff vessel and into the surrounding water for 183 days. The system was maintained at 90°C, initial pH was 8.5 and final pH was 8.8, final concentrations in the source-solution were 80 ppb U, 20 ppb  $^{239}\text{Pu}$ , 0.05 ppb  $^{237}\text{Np}$ , and 30 ppb  $^{99}\text{Tc}$ . The outer solution had final concentrations of <.05 ppb U, <.001 ppb  $^{239}\text{Pu}$ , <  $10^{-5}$  ppb  $^{237}\text{Np}$ , and 0.7 ppb  $^{99}\text{Tc}$ . At the end of the experiment, the solutions were removed from the tuff vessel and it was allowed to air dry at room temperature. The floor of the tuff vessel was removed by dry-coring, sectioned and prepared for analysis.

The tuff-wafer and tuff-cup pieces were sectioned with a diamond-blade saw to expose the interior (Fig. 1). Maps of the 0.01-1 cm pore structure were made with an optical microscope and image analysis package. Secondary (SEM) and back-scattered (BSE) electron imaging and image analysis of the tuff samples allowed high-resolution examination of large areas on the samples and helped identify mineralogy, pore structure, and the presence of micro-fractures. The size distribution of connected pores in the tuff wafer was also obtained with mercury-intrusion porosimetry. Isotope abundances were measured in the tuff with a CAMECA IMS-3f secondary ion mass spectrometer (SIMS) equipped with a resistive anode encoder (RAE) detector. Analysis was made in the step-scan mode both perpendicular and parallel to the direction of diffusive transport in the tuff (Fig. 1) using either 50  $\mu\text{m}$  or 100  $\mu\text{m}$  steps and 100  $\mu\text{m}$  x 100  $\mu\text{m}$  scan sizes to obtain a continuous profile. Surface roughness does not effect step-scan profiles as the roughness scale is much less than the analysis depths. Analyses were also made in the depth mode for the tuff wafer and a section of the tuff-cup sample. In this mode, abundance vs. depth was measured on 60  $\mu\text{m}$  x 60  $\mu\text{m}$  areas (selected randomly in areas of fine-grained matrix on the surface that was exposed to radiotracers) every 0.1  $\mu\text{m}$  in the upper 20  $\mu\text{m}$ . Corrections were made for surface effects<sup>1</sup> on the tuff-wafer while excessive roughness on the tuff-cup precluded some measurements. The distribution of  $^{239}\text{Pu}$ ,  $^{238}\text{U}$ ,  $^{235}\text{U}$ ,  $^{237}\text{Np}$ ,  $^{232}\text{Th}$ ,  $^{7}\text{Li}$ ,  $^{30}\text{Al}$ ,  $^{92}\text{Zr}$ ,  $^{11}\text{B}$ ,  $^{24}\text{Mg}$ ,  $^{40}\text{Ca}$ , and  $^{140}\text{Ce}$  were measured as appropriate.

## Tuff wafer experiment



## Tuff cup experiment

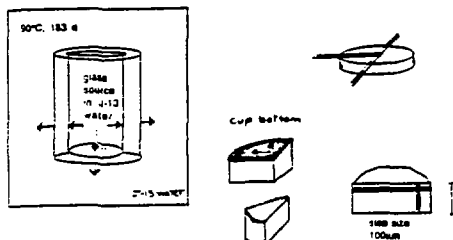


Figure 1. Schematic of tuff wafer and tuff-cup vessel showing location of SIMS analysis for radiotracers and trace elements. Polished surfaces are shown by shading, step-scan analysis locations with heavy lines, and depth mode analysis locations with heavy dots.

## RESULTS AND DISCUSSION

The concentration of tracer  $^{235}\text{U}$  measured in the interior of tuff wafer (1 mm from the diffusion surface) varied by up to a factor of 10 over the 9 mm path length that was sampled (Fig. 2a), with higher  $^{235}\text{U}$  values corresponding to areas of greater porosity in the tuff (Fig. 2b). In the tuff cup, regions also occurred where the radiotracers  $^{238}\text{U}$ ,  $^{239}\text{Pu}$ , and  $^{237}\text{Np}$  occurred at significantly higher concentrations than the mean (Fig. 3). Values for  $^{239}\text{Pu}$  and  $^{237}\text{Np}$  varied by nearly 2 orders of magnitude over the 16 mm that were sampled parallel to the surface while  $^{238}\text{U}$  concentrations varied by up to a factor of 20 across this region. The  $^{239}\text{Pu}$  and  $^{237}\text{Np}$  do not occur naturally in the tuff so their presence must be attributed entirely to diffusive transport and sorption in the tuff. Regions where  $^{238}\text{U}$  is enhanced in the tuff by diffusion from the actinide-glass source solution can be identified by levels markedly above background (which was measured on blanks) and by elevations in the  $^{238}\text{U}/^{232}\text{Th}$  ratio. The elevated concentrations of all the tracers at 6 mm and at 10.5 mm in the tuff-cup experiment are clearly due to enhanced transport into the tuff in regions of greater than average porosity.

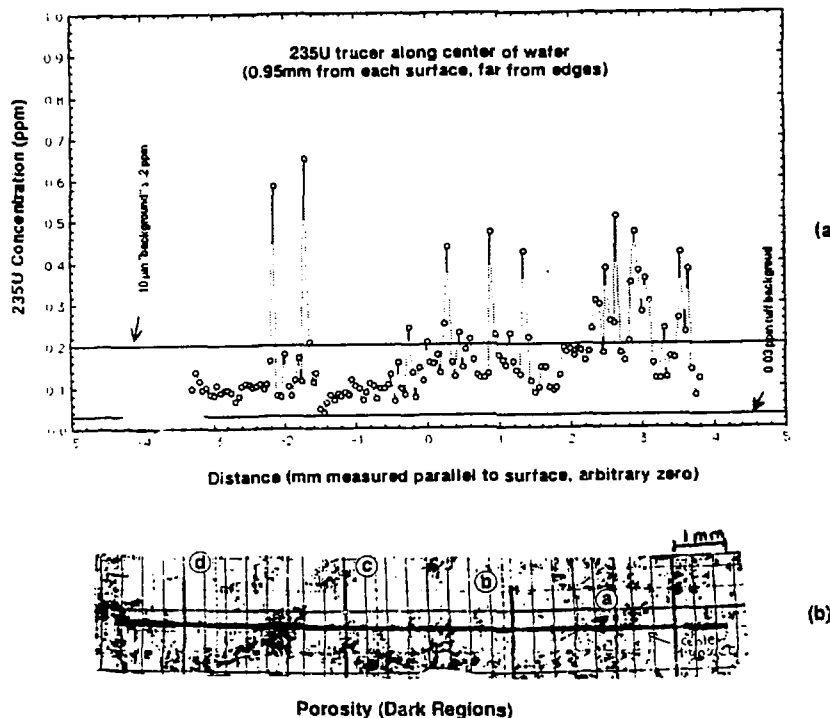


Figure 2.(a)  $^{235}\text{U}$  concentrations in the wafer interior. The circled values may be low due to a sample-holder-edge artifact. Note that  $^{235}\text{U}$  at most points measured is well above background levels of 0.03 ppm for this tuff. (b) Porosity in wafer interior, shown at the same distance scale as  $^{235}\text{U}$  distribution. Darker regions indicate larger pores and represent the 3-5% of the total pore volume that has equivalent pore diameters of 10-100  $\mu\text{m}$ . The line in the center is the SIMS analysis track corresponding to (a) and the dashed lines labelled with the letters a-d on the porosity image indicate locations of step scans taken perpendicular to the surface.

### Transect in interior of tuff cup (183 d)

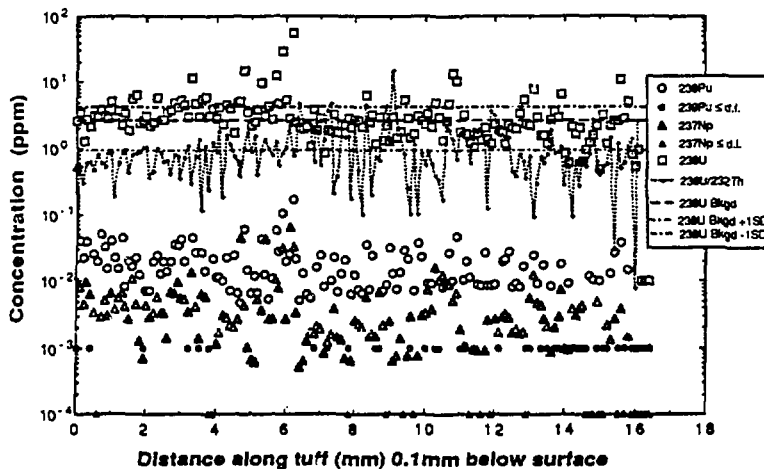


Figure 3.  $^{238}\text{U}$ ,  $^{239}\text{Pu}$ , and  $^{137}\text{Np}$  concentrations in the tuff cup interior. The analysis region was parallel the diffusive surface approximately 100  $\mu\text{m}$  below the surface. Points where  $^{239}\text{Pu}$  and  $^{237}\text{Np}$  were below the detection limit are shown as smaller symbols.  $^{238}\text{U}$  background values ( $\pm 1$  standard deviation) are shown by dashed lines.  $^{238}\text{U}/^{232}\text{Th}$  concentration ratios and  $^{238}\text{U}/^{92}\text{Zr}$  abundance ratios (arbitrary units) are also given.

Apparent diffusion coefficients ( $D_{\text{app}}$ ) calculated from  $^{235}\text{U}$ -concentration-vs.-depth profiles depended on the time and scale (mm or  $\mu\text{m}$ ) over which concentration gradients were measured, in the heterogeneous Topopah Spring tuff<sup>5</sup>. Values ranged from  $\sim 10^{-12}$  to  $\leq 10^{-18}$   $\text{cm}^2/\text{s}^{1.4}$  (1 m to 182 d exposure) in the upper 20  $\mu\text{m}$  of tuff wafers<sup>1,4</sup> to  $\sim 10^{-8}$  to  $10^{-9}\text{cm}^2/\text{s}$  in the wafer interior (8 hr exposure). This scale effect is illustrated in Fig. 4 which shows  $^{235}\text{U}$  concentrations vs depth measured every 0.1  $\mu\text{m}$  at the surface of the wafer and those measured every 50  $\mu\text{m}$  in the interior. There are two populations of pore-size in these samples (Fig. 5a); approximately 97% of the pore volume occurs in pores with an equivalent diameter less than 1  $\mu\text{m}$  (mean 0.3  $\mu\text{m}$ ) while approximately 3% of the pore volume is in pores of 10-100  $\mu\text{m}$  equivalent diameter. Image analysis of SEM photo-micrographs showed that the smaller pores are randomly oriented in the matrix while the larger pores occur in patches (Fig. 5b). The transport of  $^{235}\text{U}$  into the interior of the tuff wafer occurred in the regions of greater porosity (Fig. 2), hence the concentration vs. depth profile of  $^{235}\text{U}$  in the wafer interior was used to calculate a  $D_{\text{app}}$  of  $10^{-9}$  to  $10^{-8}\text{ cm}^2/\text{s}$  in the "high-porosity" region. This value was assumed for 3% of the pore volume, its contribution to the tracer concentration subtracted from the near-surface profiles and a  $D_{\text{app}}$  of  $5 \times 10^{-13}$  to  $5 \times 10^{-12}\text{ cm}^2/\text{s}$  determined for the 97% pore volume in the "matrix". The agreement between the data and this dual-porosity model (Fig. 4) of  $^{235}\text{U}$  diffusive transport into the tuff confirms that a small but significant amount of the tracer is transported much faster in the porous regions than would be predicted from a homogeneous porosity model. The time-dependency of  $D_{\text{app}}$  is then an artifact of assuming a heterogeneous medium. It is particularly necessary to consider heterogeneous porosity when predicting transport rates because >95% of actinide transport occurs in the matrix (slow) and ~5% occurs in microfractures (up to 1000 x faster) in saturated diffusive systems while in unsaturated advective systems most transport will occur in microfractures at the faster rate. In unsaturated systems, transport will occur in microfractures (fast) only during high-flow rates while transport will generally occur in the matrix (slow) and along capillary films. Use of the actual multi-modal pore-distribution spectrum would provide further insight into the rates of transport controlled by the scale of physical structure in the heterogeneous rock.

## 235U transport into tuff wafer

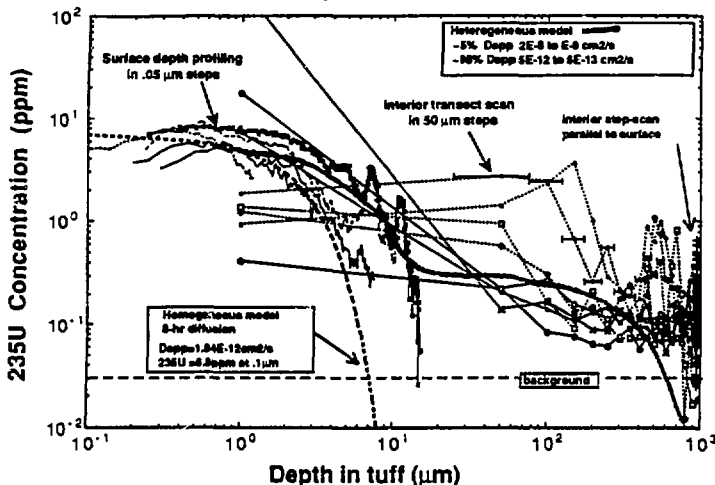


Figure 4.  $^{235}\text{U}$  concentrations vs. depth obtained from surface depth profiles (lines with no symbols), interior step-scans perpendicular to the surface (lines with symbols), and interior step-scans parallel to the surface (crosses) on a wafer exposed to  $^{235}\text{U}$  for 8 hours in a static-diffusion experiment. Different line patterns or symbols indicate separate analysis locations. Model fits are shown in bold lines. The values shown in Fig. 2a are plotted here at 1 mm depth.

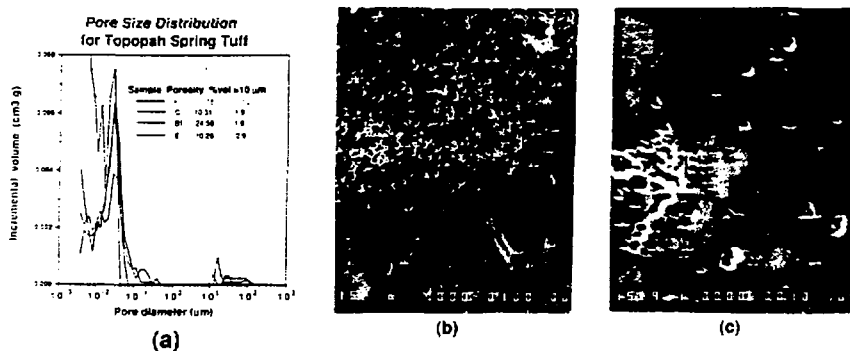


Figure 5. (a) Pore-size distribution in Topopah Spring Tuff determined from mercury-intrusion porosimetry. (b) SEM photo-micrograph of tuff wafer at 160x magnification showing the  $> 10 \mu\text{m}$  pores and at (c) 900x magnification showing the smaller pores. Scale bars of 100  $\mu\text{m}$  (a) and 10  $\mu\text{m}$  (b) are included.

The solution chemistry, actinide source, temperature, transport time, and water/rock ratio in the tuff-cup experiment were closer to those expected in the proposed Yucca mountain repository than in the wafer experiment. We saw (Fig. 3) that there was indeed greater actinide penetration into some regions of the tuff cup than others. A concentration profile taken at 100  $\mu\text{m}$  depth intervals from the surface to 7 mm into the tuff-cup (Fig. 6), however, did not produce a curve adequate for modeling the a  $D_{\text{app}}$  in the porous regions. Only one estimate of  $\leq 10^{-11} \text{ cm}^2/\text{s}$  could be made since just the uppermost points for  $^{239}\text{Pu}$  and  $^{238}\text{U}$  concentrations had clear enhancements of these species relative to the interior. Furthermore, the frequent spikes of  $^{238}\text{U}$  and  $^{239}\text{Pu}$  throughout the analyzed 7 mm show greater transport in some regions than others. The fact that these peaks are essentially the same height indicates that communication between the solution and the interior of the wafer along these faster transport paths may have attained an equilibrium during the 183 days of exposure to the radiotracer solution. Comparison with the  $^{238}\text{U}/^{92}\text{Zr}$  and the  $^{238}\text{U}/^{232}\text{Th}$  ratios measured at the same time confirm that these enhanced  $^{238}\text{U}$  values are indeed due to input from the actinide-glass source solution and not to any inherent variations in the background  $^{238}\text{U}$  of the tuff.

#### Tuff cup (183d) step-scan from surface to interior

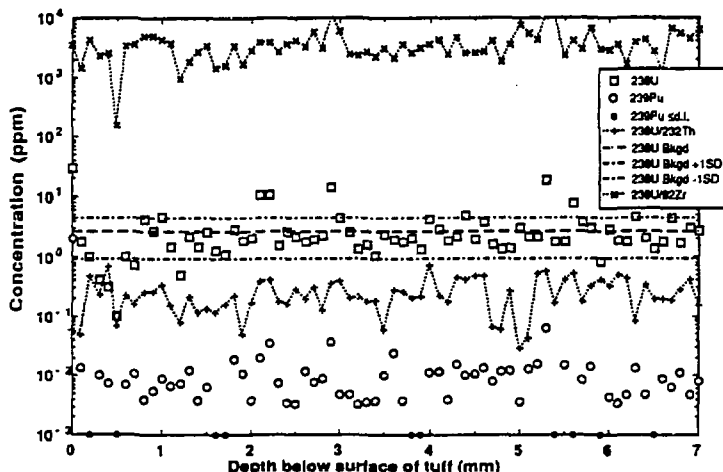


Figure 6.  $^{238}\text{U}$  and  $^{239}\text{Pu}$  concentrations in the upper 7 mm of the tuff cup interior. Analysis was in the floor of the tuff-cup, perpendicular to the direction of diffusive transport, and each data point integrates over a  $100 \mu\text{m} \times 100 \mu\text{m}$  area.

A second set of concentration vs. depth profiles in the tuff cup was taken using the depth-profiling mode on the SIMS. The analysis at 0.1  $\mu\text{m}$  depths in the upper 10  $\mu\text{m}$  of a sample was again inadequate to calculate a  $D_{\text{app}}$  for the matrix of the tuff cup. The interior floor of the tuff-cup vessel was initially too rough ( $> 10 \mu\text{m}$  relief) for SIMS depth-profiling so one section was polished prior to SIMS analysis. Polishing can remove up to 30  $\mu\text{m}$  of the surface exposed to radiotracer. As seen in Fig. 7, most of the elevated tracer concentrations were removed with the polished surface, and transport rates were insufficient to produce a concentration gradient beyond the remaining uppermost 0.5 micron (not shown). Additional concentration-vs.-depth profiles need to be measured in replicate on an unpolished section in order to generate, after surface effect corrections<sup>1</sup>,  $D_{\text{app}}$  values for the matrix regions of the tuff in this experiment. Preliminary results from one depth-scan, however, suggest a value of  $10^{-15}$ - $10^{-16} \text{ cm}^2/\text{s}$ .

### Tuff cup (183 d) depth-scan on polished interface

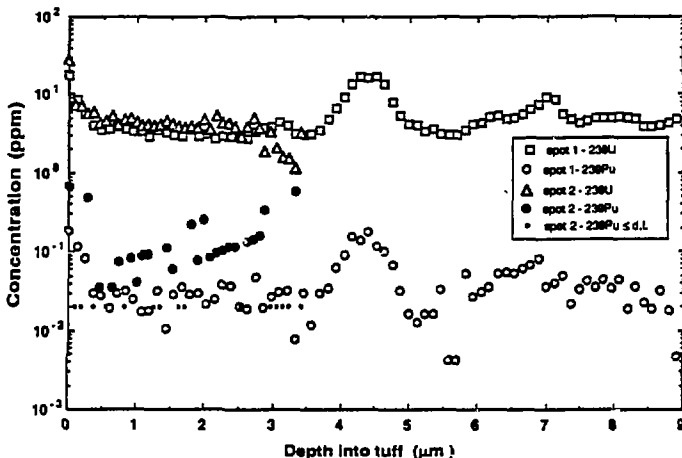


Figure 7.  $^{238}\text{U}$  and  $^{239}\text{Pu}$  concentrations in the upper 9  $\mu\text{m}$  of a section of the tuff cup. Polishing of this section prior to analysis probably removed the uppermost 30  $\mu\text{m}$  of the sample so that little remains of the concentration vs. depth profile developed for these isotopes at the interface.

Comparison of the concentration profiles and apparent diffusion coefficients obtained in the 8-hour tuff-wafer experiment with those obtained in the 183-day tuff-cup experiment indicate that net transport was somewhat slower in the tuff-cup experiments. The  $D_{\text{app}}$  incorporate effects of molecular diffusivity, tortuosity, retardation due to sorption or precipitation in the rock, and the influence of colloids on mobility due to enhanced "solubility" or filtration. Differences in these two systems, the tuff-cup and the tuff-wafer experiments, must be attributed to differences in one or all of these conditions. Both systems had enhanced transport in a small fraction of the rock that had greater porosity than the bulk of the sample. The higher bicarbonate in the tuff-wafer experiments produced U-carbonate complexes that increased the solubility of uranium<sup>6</sup> and slightly lowered sorption ( $K_d$  values) for  $^{235}\text{U}$  onto tuff. The actinides in the glass-source solution occur both as dissolved species and as colloidal ( $< 0.4 \mu\text{m}$ ) particles. Alteration products form during glass leaching, often resulting in layers of clay minerals spalling from the glass surface<sup>7</sup>. In solution, these particles may contain the actinides or actinides in solution may become sorbed to them. In addition, naturally occurring colloids or organic macromolecules present in J-13 groundwater may adsorb radioisotopes or aggregate glass-alteration products. Particles and colloids have been identified both in J-13 water<sup>8</sup> and in the glass-leach solution from this tuff-cup experiment<sup>9</sup>. The 10-100  $\mu\text{m}$  pores existing in the Topopah tuff are clearly large enough to provide channels for transport of dissolved species and some of these particles. The bulk of transport in the tuff wafers, however, was found to occur in the finer-grained matrix where 95% of the pore volume resides. Consequently, it is likely that colloidal species present in the solutions are filtered out during migration through this tortuous region with mean pore diameter of .03  $\mu\text{m}$ . It is likely that a greater percentage of the actinides from the glass solution are in particulate or colloidal form than in the bicarbonate solution, hence, the greater efficiency of removal of actinides from the mobile phase by filtration could account for much of the difference in transport rates found in these experiments.

## SUMMARY

- 1) Regions of faster actinide transport occur in porous areas of Topopah Spring Tuff to depths of 1 mm in 8-hour and 7 mm in 183-day static diffusion experiments.
- 2) Porous regions of the tuff account for less than 5% of the pore volume in the tuff.
- 3) Most of the net actinide transport in saturated tuff occurs in the matrix (<10  $\mu\text{m}$  equivalent pore diameter) at apparent diffusion rates up to 3 orders of magnitude slower than in the porous regions.
- 4) Filtration of colloidal particles in the fine-grained matrix of Topopah Spring Tuff may result in slower actinide transport rates for solutions where larger fractions of the actinides are associated with suspended particulates or colloids, e.g., glass-leach solutions.

## ACKNOWLEDGEMENTS

We thank James Wong, Joan Beiriger, Kevin McKeegan, Ron Pletcher and Virginia Oversby for technical assistance in various aspects of this study. Prepared by Yucca Mountain Site Characterization Project (YMP) participants as part of the Civilian Radioactive Waste Management Program. The Yucca Mountain Site Characterization Project is managed by the Yucca Mountain Site Characterization Project Office of the U.S. Dept. of Energy, Las Vegas, Nevada. Work performed under the auspices of the U.S. Dept. of Energy by Lawrence Livermore National Laboratory under contract No. W-7405-ENG-48.

## REFERENCES

- <sup>1</sup>McKeegan, K. D., D. Phinney, V.M. Oversby, M. Buchholtz-ten Brink, and D.K. Smith in *Scientific Basis for Nuclear Waste Management XII*, (Mat. Res. Soc. Proc. 127, Pittsburgh, PA 1989) pp. 813-821
- <sup>2</sup>F.Bazan, J. Rego, and R.D. Aines in *Scientific Basis for Nuclear Waste Management X*, edited by J.K. Bates and W.B. Seefeldt, (Mat. Res. Soc. Proceedings 84, Pittsburgh, PA 1987) pp447-458
- <sup>3</sup>F.M. Byers and L.M. Moore, Los Alamos Natl. Lab. Report No. La-10901-MS (Los Alamos, NM 1987) 72 pp.
- <sup>4</sup>K.D McKeegan, M.R. Buchholtz-ten Brink, V.M. Oversby, and D.L. Phinney, Trans. Am. Geophys. Union 68(44), 1282 (1987)
- <sup>5</sup>M.R. Buchholtz ten Brink, D. Phinney, K.D. McKeegan and V.M. Oversby, presented at *Chemistry and Migration Behavior of Actinides and Fission Products in the Geosphere*, Monterey, CA, Nov. 1989 (unpublished)
- <sup>6</sup>C. Bruton, (private communication, 1989)
- <sup>7</sup>J.K. Bates, W.L. Ebert and T.J. Gerdin, in *High Level Radioactive Waste Management Proceedings*, Vol.2 , (Publ Am. Nucl. Soc., LaGrange Park, IL 1990) pp.1095-1102.
- <sup>8</sup>M.R Buchholtz ten Brink, S. Martin, B. Viani, D. Smith and D. L. Phinney, Presented at *Concepts in manipulation of groundwater colloids for environmental restoration*, Manteo, NC, Oct 15-18, 1990, Ed. J. McCarthy for proceedings in press.
- <sup>9</sup>J. Rego (private communication, 1990)